

See discussions, stats, and author profiles for this publication at: <https://www.researchgate.net/publication/264054796>

Selenadiazole derivatives as potent thioredoxin reductase inhibitors that enhance the radiosensitivity of cancer cells

ARTICLE in EUROPEAN JOURNAL OF MEDICINAL CHEMISTRY · JULY 2014

Impact Factor: 3.45 · DOI: 10.1016/j.ejmech.2014.07.032 · Source: PubMed

CITATIONS

3

READS

36

5 AUTHORS, INCLUDING:



Xiaoling li

China Three Gorges University

238 PUBLICATIONS 3,973 CITATIONS

SEE PROFILE



Wenjie Zheng

Jinan University (Guangzhou, China)

100 PUBLICATIONS 1,292 CITATIONS

SEE PROFILE



Tianfeng Chen

Jinan University (Guangzhou, China)

115 PUBLICATIONS 1,745 CITATIONS

SEE PROFILE



Original article

Selenadiazole derivatives as potent thioredoxin reductase inhibitors that enhance the radiosensitivity of cancer cells

Yuan-Wei Liang^a, Junsheng Zheng^b, Xiaoling Li^{a,*}, Wenjie Zheng^a, Tianfeng Chen^{a,*}^a Department of Chemistry, Jinan University, Guangzhou 510632, China^b The Third Affiliated Hospital of Sun-Yat-Sen University, Guangzhou 510632, China

ARTICLE INFO

Article history:

Received 14 March 2014

Received in revised form

6 July 2014

Accepted 10 July 2014

Available online 10 July 2014

Keywords:

Radiosensitization

Selenadiazole

Thioredoxin reductase

ROS

ABSTRACT

Thioredoxin system is an attractive target to overcome radioresistance in cancer therapy. The redox enzyme thioredoxin reductase (TrxR) plays a vital role in restoring cellular thiol redox balance disrupted by radiation-induced reactive oxygen species (ROS) generation and oxidative damage. In this study, a series of 1,2,5-selenadiazoles have been synthesized and identified as highly effective inhibitors of TrxR to disrupt the intracellular redox balance, and thus significantly enhanced the sensitivity of cancer cells to X-ray. Upon irradiation, 1,2,5-selenadiazoles displayed a marked synergistic inhibitory effect on radioresistant A375 melanoma cell through enhancement of ROS overproduction, and subsequent induction of ROS-promoted apoptotic pathways, which triggered then mitochondrial dysfunction and caspase activation, finally resulted in augment of radiotherapeutic efficacy. Interestingly, we also found the interaction sites between 1,2,5-selenadiazole and the model peptide of TrxR, which can be confirmed by MALDI-ToF-MS. These results clearly demonstrate TrxR as a potential target for therapy of radio-resistant cancers, and selenadiazole derivatives may be attractive radiosensitizing agent by targeting TrxR.

© 2014 Elsevier Masson SAS. All rights reserved.

1. Introduction

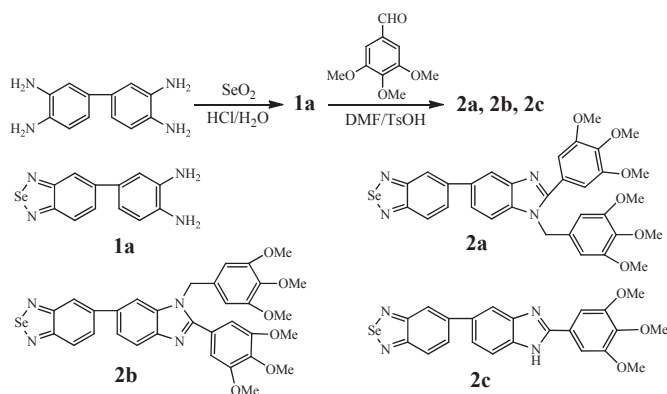
Cancer is the second leading cause of death in the world after cardiovascular diseases. Today, millions of cancer people extend their lives attributing to early identification and treatment. Although radiation therapy is well-known to play an important role in cancer treatment, the common problem of resistance remains a major obstacle worthy of exploration [1,2]. Radiation-induced ionizations may act directly on the cellular component molecules or indirectly on water molecules, causing water-derived radicals, which react with nearby molecules in a very short time, resulting in oxidation of the affected molecules [3–5]. Reactive oxygen species (ROS) generated as a result of indirect damage is the principal mediator of radiation induced damage to biological systems. Generation of ROS creates oxidative stress and disturbs redox balance within the cells, triggering up-regulation of antioxidant systems [6] which conduce to the induction of resistance mechanisms. This makes the ubiquitous redox enzyme thioredoxin reductase an

attractive drug target. In all thioredoxin system, thioredoxin (Trx) involves in redox reactions through its conserved active site with two thiol residues (–Cys–Gly–Pro–Cys–) which can be reduced by thioredoxin reductase (TrxR) using electrons from NADPH [7]. Previous works have showed that 1,2,5-selenadiazole derivatives exerted extensive biological activities against a wide variety of cancer cells [8,9]. With TrxR-inhibition as the aim, drawing on these works, three novel benzimidazole group-containing 1,2,5-selenadiazole-oriented derivatives were designed and synthesized recently and were subjected to test for inhibition efficiency and specificity on A375 human melanoma cells, which have traditionally been considered radiation resistant so that radiation therapy has not commonly been employed to treat it [10]. In the present study, a series of 1,2,5-selenadiazole derivatives (Scheme 1) were synthesized and evaluated as *in vitro* radiosensitizer on the A375 cells as well as antiproliferation agents. The underlying molecular mechanisms accounting for the synergistic effects were also elucidated.

Chemoradiotherapy (CRT), the concurrent use of radiation therapy and chemotherapy, is a well-established field that in most cases works better than just using either of them alone and, actually contributes to the improvement in the overall health of the patient as well as extending the life expectancy in some patients

* Corresponding authors.

E-mail address: tchentf@jnu.edu.cn (T. Chen).



Scheme 1. General method for the synthesis of 1,2,5-selenadiazole derivatives (**1a**, **2a**, **2b** and **2c**).

[11,12]. Decades ago, researchers introduced a theoretical framework to describe the interaction of cytotoxic chemotherapy and radiotherapy [13], called “spatial cooperation”, it proposed that the action of radiation and chemotherapeutic drugs is directed toward different target sites in the body and might interaction with each other. Radiation tends to target localized tumors, while chemotherapy drugs are likely to be more effective in eliminating micrometastases. However, relationship between radiotherapy and chemotherapeutic drugs in biological systems need to be further elucidated. In this study, a series of 1,2,5-selenadiazoles have been synthesized and identified as highly effective inhibitors of TrxR to disrupt the intracellular redox balance, and thus significantly enhanced the sensitivity of cancer cells to X-ray. Upon irradiation, 1,2,5-selenadiazoles displayed a marked synergistic inhibitory effect on radioresistant A375 melanoma cell through enhancement of ROS overproduction, and subsequent induction of ROS-promoted apoptotic pathways, which triggered then mitochondrial dysfunction and caspase activation, finally resulted in augment of radiotherapeutic efficacy. Taken together, these results clearly demonstrate TrxR as a potential target for therapy of radioresistant cancers, and selenadiazole derivatives may be attractive radiosensitizing agent by targeting TrxR.

2. Results and discussion

2.1. Chemistry

In terms of the synthesis of 1,2,5-selenadiazole derivatives, **1a** was synthesized by 3,3'-Diaminobenzidine (214 mg, 1 mmol) and selenium dioxide (111 mg, 1 mol) in 0.2 N HCl. Importantly, the following condensation reaction of **a** and 3,4,5-Trimethoxybenzaldehyde (molar ratio: 1:1.2) which catalyzed by p-TSA using DMF as solution with aim of introduction of benzimidazoles group ultimately gained three products (Scheme 1). This is different from previous literatures [14] in terms of classical condensation reaction of o-phenylenediamine with aldehydes, which mostly acquired only one or two products. **2a** and **2b** are isomerides which were further separated by HPLC (Agilent Edipse XDB-C18, 21.2×250 mm, $7 \mu\text{m}$) using water and acetonitrile (from 72:28 to 36:64, 8.0 ml/min) as mobile phase and ultraviolet as detector (320 nm).

2.2. In vitro anticancer activities of selenadiazoles in combination with X-ray

The antiproliferative activities of the 1,2,5-selenadiazole (**2a**, **2b** and **2c**) alone or in combination with X-ray (8 Gy) were firstly

screened against A375 cells by means of MTT assay (Fig. 1A, B and C). The results showed that CRT had significantly greater inhibitory effects than using corresponding radiotherapy or chemotherapy alone on A375 cells. IC_{50} value of **2a**, **2b** and **2c** (Fig. 1D) reduced from 28.3 $\mu\text{g}/\text{ml}$, 26.4 $\mu\text{g}/\text{ml}$, 12.4 $\mu\text{g}/\text{ml}$ to 9.2 $\mu\text{g}/\text{ml}$, 8.0 $\mu\text{g}/\text{ml}$ and 2.2 $\mu\text{g}/\text{ml}$ (18 h) respectively after combining with 8 Gy. Apparently, the dosage of agents decreased greatly, so that systemic toxicity was considerably lowered down while the anti-proliferative activities of the agents were highly enhanced. Agents have brought great alteration into the IC_{50} value, especially for **2c**, which in combination with 8 Gy was only approximately one sixth (1/6) of free **2c**. In addition, **2a** and **2b**, which are structural isomerides and have extreme similarity in the chemical structure bore a remarkably close resemblance to each other in the inhibitory effect on cell viability. Morphological examination of the cells (Fig. 1E) after corresponding treatment showed the typical feature of cell death such as cell shrinkage and rounding up of the cells. Noteworthy, The structure of **2a**, **2b** or **2c** remained the same after irradiation.

Anticancer drugs exert at least part of their cytotoxic effect by triggering apoptosis in susceptible cells [15]. Therefore, flow cytometric analysis were performed to determine whether apoptosis was involved in cell death induced by 1,2,5-selenadiazoles and corresponding CRT. As shown in Fig. 2A and Sub-G1 cell populations (see Supporting information), there was hardly any apoptosis observed in A375 cells which exposed to 8 Gy alone without treatment with **2b** or **2c**, just 2.3%. Nevertheless, treatment with **2b** (10 $\mu\text{g}/\text{ml}$) alone only triggered 11.7% of apoptotic cells, amazingly, in the presence of 8 Gy, this section substantially increased to 57.6%. Likewise, treatment with **2c** (4 $\mu\text{g}/\text{ml}$), the proportion of apoptotic cells rose from 36.2% in the absence of 8 Gy to 57.1% in the presence of 8 Gy. This apparently indicated that in the presence of 8 Gy, they significantly increased the apoptosis-inducing effect in comparison with that in the absence of 8 Gy and definitely the apoptosis is the major mode of cell death induced by **2b** or **2c** in the absence or presence of 8 Gy.

2.3. Compounds (**2b/2c**) in combination with 8 Gy enhance the apoptosis-inducing effect

There are two main apoptotic pathways: the extrinsic or death receptor pathway and the intrinsic or mitochondrial pathway [16]. Each requires specific triggering signals to begin an energy-dependent cascade of molecular events. Since that CRT could significantly amplify the *in vitro* anticancer and apoptosis-inducing effects of **2b** or **2c**, we subsequently conducted further experiments to understand the molecular mechanism.

Caspases, closely associated with apoptosis, are aspartate-specific cysteine proteases and members of the interleukin-1 β -converting enzyme family [17]. The caspase-cascade system plays central roles in the induction, transduction and amplification of intracellular apoptotic signals. In this study, activation of two initiator caspases: caspase-8 (Fas/TNF-mediated) caspase-9 (mitochondrial-mediated), and an executor caspase caspase-3 were therefore measured by fluorometric assay for the apoptotic program. Fig. 2B indicated that Exposure of A375 cells to **2c** (2 $\mu\text{g}/\text{ml}$) alone can increase the activation of caspase-3/8/9, resulted in the involvement of both intrinsic and extrinsic apoptotic pathways. Furthermore, treatment of **2c** in the presence of 8 Gy apparently enhanced the activation caspase-3/8/9 to a higher degree. These results were further confirmed by caspases and cleavage of PARP as examined by Western blotting. As shown in Fig. 2C, exposure of A375 cells to **2c** in the absence or presence of 8 Gy both caused increase in the activation of caspase-3, caspase-8 and caspase-9, and apparently the latter way was more noticeable,

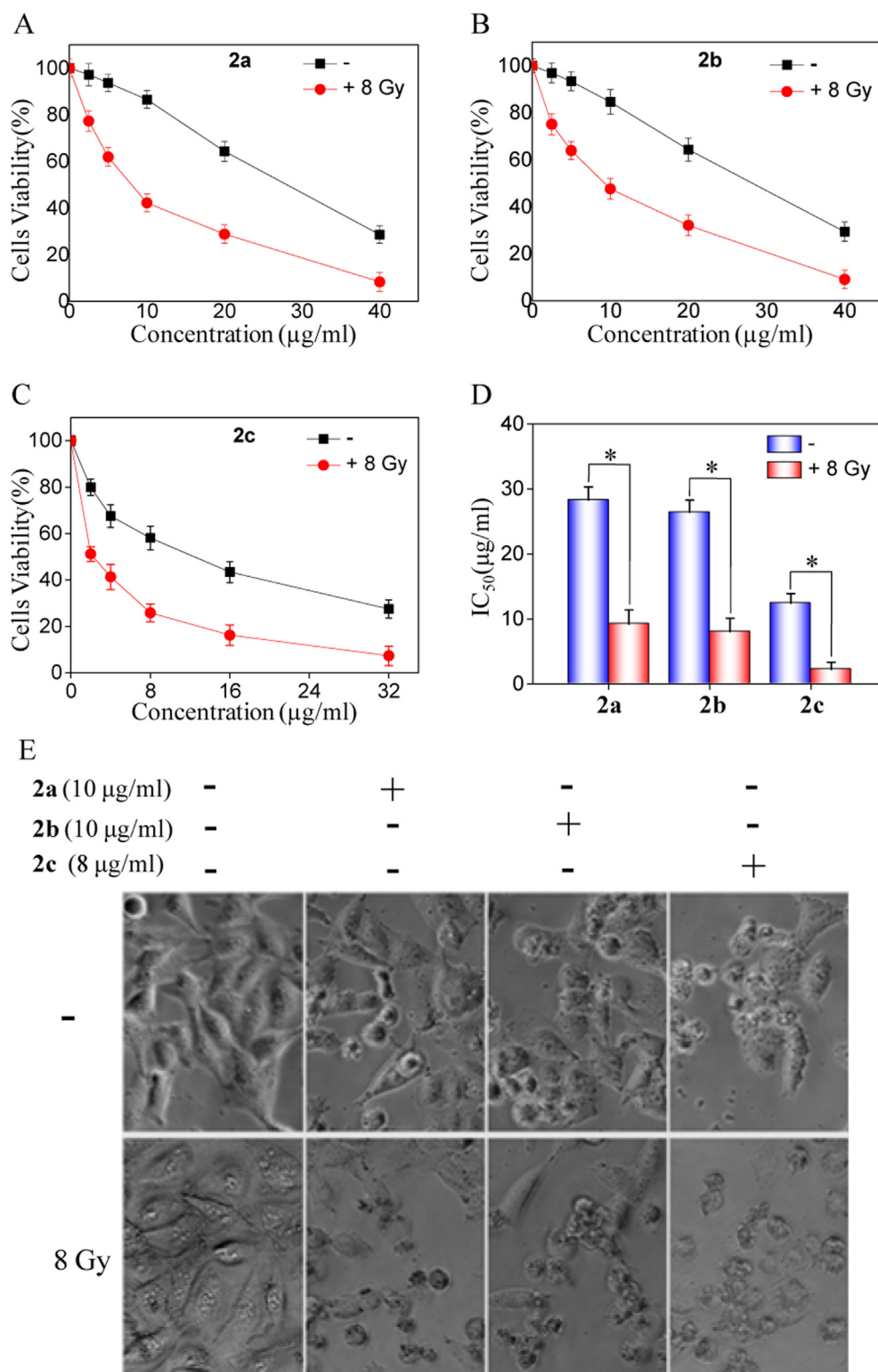


Fig. 1. Compounds **2a**, **2b** and **2c** treatment effects on A375 cell viability in the absence or presence of 8 Gy. (A), (B), (C) Growth inhibition of compounds (**2a**, **2b**, **2c**) alone or combined with 8 Gy on A375 cells. A375 cells were treated increasing concentrations of compounds (**2a**, **2b**, **2c**) for 6 h then were exposed or unexposed to 8 Gy irradiation and further incubated for 12 h. Cell viability was determined by MTT assay. (D) IC₅₀ value of **2a**, **2b** and **2c**. (E) Representative images of A375 cells under different treatments. Cells were pretreated with individual agent for 6 h, exposed or unexposed to 8 Gy and further incubated for another 12 h. Bars with different characters are statistically different at **P* < 0.05.

resulting in induced the proteolytic cleavage of PARP, a protein serving as a biochemical hallmark of cells undergoing apoptosis. Treatment of A375 cells with **2c** in the presence of 8 Gy led to the decrease in the level of full-length PARP and substantially with

concomitant increase in the level of cleaved PARP. These results demonstrated that both the extrinsic and intrinsic pathways were involved in the CRT (**2c** + 8 Gy) treatment-induced apoptosis in A375 cells.

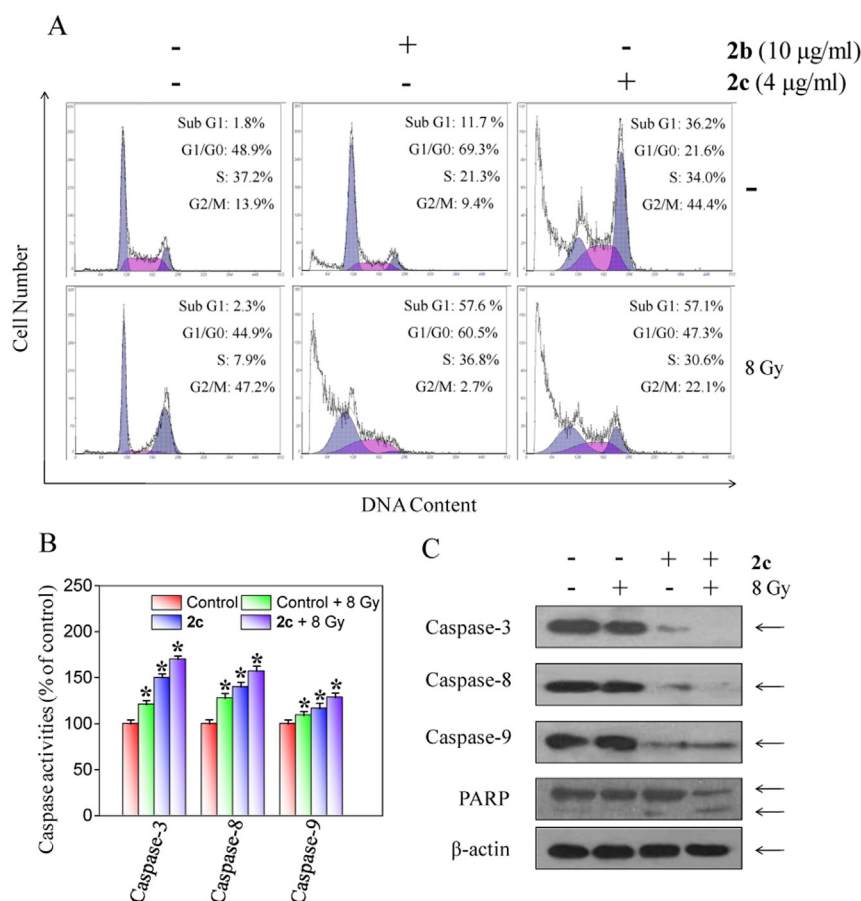


Fig. 2. Induction of cancer cell apoptosis by **2b** or **2c** alone or in combination with 8 Gy. (A) Flow cytometric analysis of A375 cells exposed to **2b** or **2c** in the absence or presence of 8 Gy. (B) Activation of Caspase-3/8/9 in A375 cells treated with compound **2c** or corresponding CRT for 18 h. (C) Western blot analysis of expression levels of Caspases activation and PARP cleavage in A375 cells treated with **2c** (2 µg/ml) or corresponding CRT for 18 h. Equal loading was confirmed by stripping immunoblots and reprobing for β-actin. All cells were pretreated with definite concentration of **2b** or **2c** for 6 h, exposed or unexposed to 8 Gy and further incubated for another 12 h. Significant difference between treatment and control groups is indicated at $P < 0.05$ (*) level.

2.4. Compound **2c** trigger mitochondria dysfunction in the presence of 8 Gy

Mitochondria play a crucial role in regulating cell death. Mitochondrial membrane potential ($\Delta\psi_m$) is an important parameter of mitochondrial function and an indicator of cell health [18]. Depletion of $\Delta\psi_m$ suggests the loss of mitochondrial membrane integrity reflecting the initiation of the proapoptotic signal, in response to many mechanistically diverse pro-apoptotic triggers, mitochondria release multiple pro-apoptotic effectors from their inter-membrane space. The control and regulation of these apoptotic mitochondrial events occurs through members of the Bcl-2 family of proteins. The Bcl-2 family of proteins governs mitochondrial membrane permeability and can be either pro-apoptotic, such as Bax, Bak, Bid, or anti-apoptotic, such as Bcl-2, Bcl-x, Bcl-XL. These proteins have special significance since they can determine if the cell commits to apoptosis or aborts the process. Hence, we examined the effects of **2c** in the absence or presence of 8 Gy on the expression levels of anti-apoptotic and pro-apoptotic Bcl-2 family proteins in A375 cells by Western blotting. As shown in Fig. 3A, treatments of the cells with **2c** alone increased the total expression levels of the pro-apoptotic protein Bax and cleavage of Bid, yet decreased the expression level of anti-apoptotic protein Bcl-2. Moreover, treatment of cells with **2c** in the presence of 8 Gy substantially increased the expression levels of Bax and down-regulated Bid and Bcl-2

expression. Thus, down-regulation of Bcl-2, up-regulation of Bax and activation of Bid could be important mechanisms by which **2c** induces mitochondria-mediated apoptosis in A375 cells.

2.5. Involvement of MAPKs pathways induced by compound **2c** combined with 8 Gy

The MAPK signaling pathway plays a key role in the regulation of gene expression, cellular growth, and survival [19]. In this study, The role of p-JNK and p38 MAPK activities in signaling pathways induced by **2c** alone or combined with 8 Gy were examined by western blot analysis. As shown in Fig. 3B, exposing A375 cells to **2c** alone can cause a gently increase in p-JNK and p38 in the treated cells, more importantly, the expression of p-JNK and p38 considerably increased after treated with **2c** in the presence of 8 Gy. These results demonstrated that activation of both p-JNK and p38 play critical role in the **2c**-induced (especially in the presence of 8 Gy) apoptosis in A375 cells.

To study the role of MARK activation on **2c** induced growth inhibition, A375 cells were subjected to specific MARK inhibitors before treated with **2c** to examine the effects. The results of MTT assay showed that pretreatment with SP600125 (JNK inhibitor) did not have effect on the **2c**-induced cell death (Fig. 3C), suggesting that p-JNK did not play important role in governing cell death induced by **2c**. However, pretreatment with SB258530 (p38

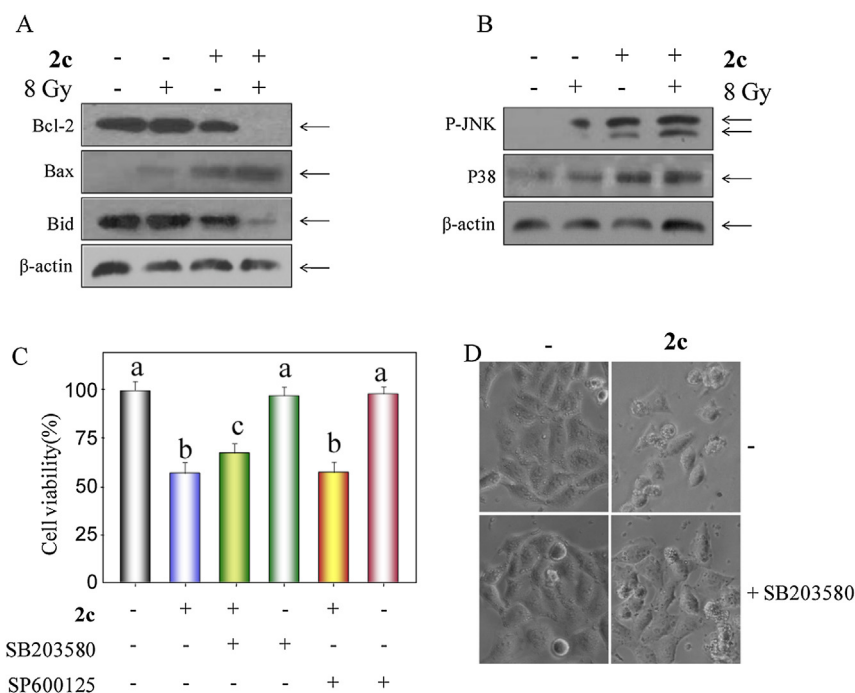


Fig. 3. Effects of **2c** in combination with 8 Gy on the expression level of Bcl-2 family proteins and MAPK signaling pathways. (A) Western blot analysis of Bcl-2 family protein. Cells were pretreated with 4 μ g/ml **2c** for 6 h, exposed or unexposed to 8 Gy and back to another 12 h incubation. (B) The phosphorylation status of JNK and expression levels of p38 MAPK after treatment of **2c** alone or combined with 8 Gy. (C) Effects of SP600125 (JNK inhibitor) and SB203580 (p38 inhibitor) on 2c-induced growth inhibition. Cells were pretreated with 20 μ M of different inhibitors 1 h prior to the treatment of 8 μ g/ml **2c** for 18 h. Cell viability was determined by the MTT assay as described in the experimental section. (D) Morphology of A375 cells after different treatment.

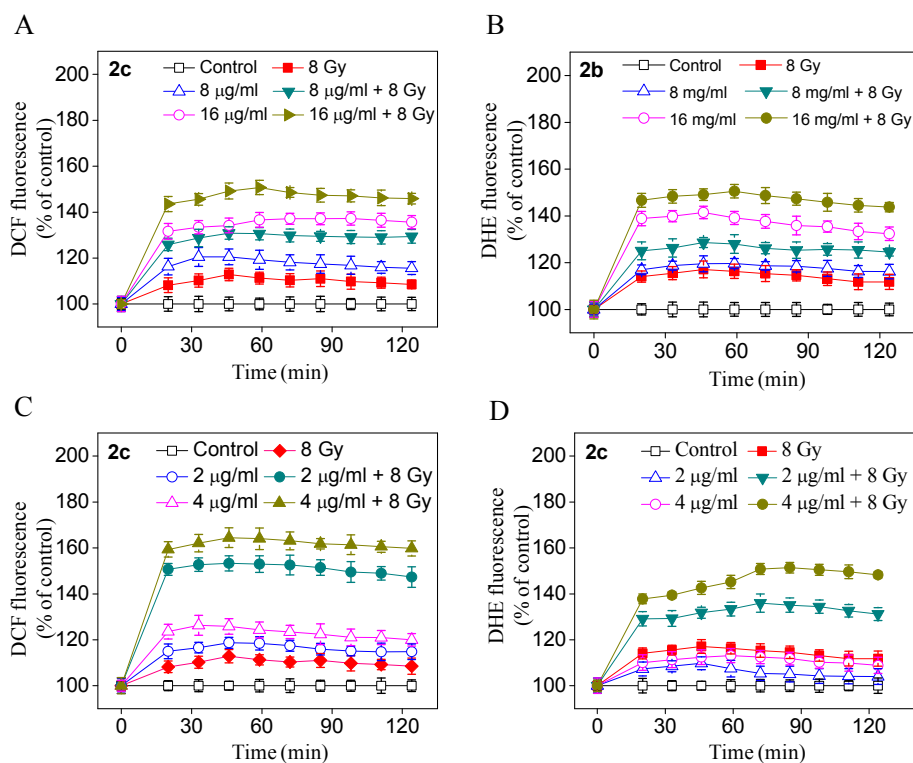


Fig. 4. The role of intracellular ROS generation in A375 cell apoptosis induced by **2b** or **2c** in the absence or presence of 8 Gy. (A), (B), (C), (D) Intracellular ROS levels measured by DCF or DHE fluorescence. A375 cells were pretreated with **2b** (8 or 16 μ g/ml) or **2c** (2 or 4 μ g/ml) for 6 h, subjected to 0 Gy or 8 Gy X-irradiation, then incubated with H_2DCF or DHE and back to incubation for 30 min at 37 $^{\circ}C$.

inhibitor) resulted in a marked decline in the proportion of dead cells. Also, the microscopic examination showed that SB258530 indeed reduced the **2c**-induced microscopic changes on cell death, like cell shrinkage and cell rounding (Fig. 3D). These suggested the involvement of activation of p38 pathway in the apoptosis of A375 cells induced by **2c**.

2.6. ROS-dependent apoptosis induced by cooperative treatment

Reactive oxygen species (ROS), as it has come to be known, is a collective term that broadly describes O₂-derived free radicals, plays an essential role in cancer cell apoptosis induced by anticarcinogenic agents that cause DNA damage in the cell nucleus. Cells react rapidly to redox imbalance with a plethora of biological responses, including cell cycle-specific growth arrest, gene transcription, initiation of signal transduction pathways and repair of damaged DNA. These early events are likely to determine whether a cell will necrose, senesce, apoptose or survive and proliferate [20].

Therefore, in this study, we investigated ROS generation in the A375 cells by measuring the DCF and DHE fluorescence intensity. The results showed that exposing A375 cells to X-ray or 1,2,5-selenadiazoles alone can trigger ROS generation moderately. Importantly, combination of X-ray and 1,2,5-selenadiazoles significantly enhanced 1,2,5-selenadiazoles-induced ROS generation (Fig. 4). These results reveal that combination of X-ray and 1,2,5-selenadiazoles can effectively induce cancer cell apoptosis in a ROS-dependent manner.

2.7. Compound **2c** induced cell apoptosis by targeting TrxR

Thioredoxin reductase (TrxR) system is associated with cancer cell growth and anti-apoptosis process. TrxR plays a vitally significant role in regulating cellular redox homeostasis. Ionizing radiation induced alteration in redox homeostasis can up-regulate of antioxidant systems and conduce to the induction of resistance mechanisms. This is likely to made TrxR to be a new potential target [21]. Hence, Aiming to investigate the effects of **2c** on redox modulation by inhibition of TrxR. The insulin reduction assay was performed. As Fig. 5A revealed, exposing A375 cells to 8 Gy can cause slightly increase in the activities of TrxR, this can subsequently restore cellular redox equilibrium in A375 cells and thus contribute to inhibition of oxidative injury, resulting in the radioresistance. On the contrast, treated cells with **2c** significantly decreased TrxR activity. This can deter TrxR from providing protection against ROS-mediated cytotoxicity. Accumulated reactive oxygen species and dysregulation might ultimately lead to apoptosis in radioresistant A375 cells. Moreover, **2c** in combination with 8 Gy caused comparatively high decrease in TrxR activity. In addition, Western

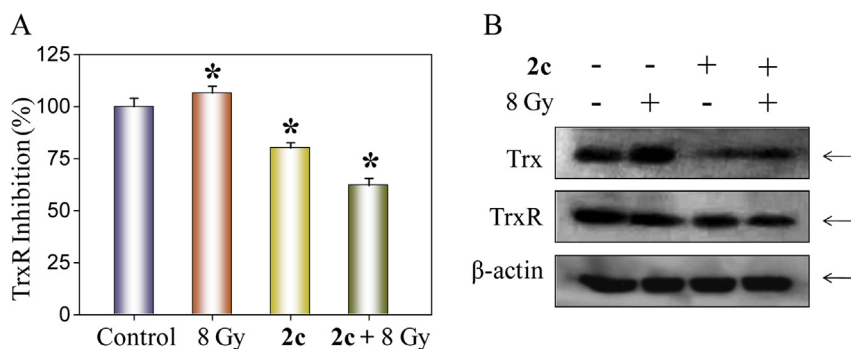


Fig. 5. Alteration of antioxidant enzyme activities of TrxR in A375 cells induced by **2c** alone or in combination with 8 Gy. (A) Enzymatic activity of TrxR in A375 cells after treatment with **2c** in the absence or presence of 8 Gy exposure. Cells were pretreated with **2c** (2 μ g/ml) for 6 h, exposed or unexposed to 8 Gy then further incubated for another 12 h. (B) Cell lysates were subjected to Western blot analysis, protein levels of TrxR and Redox thioredoxin were examined.

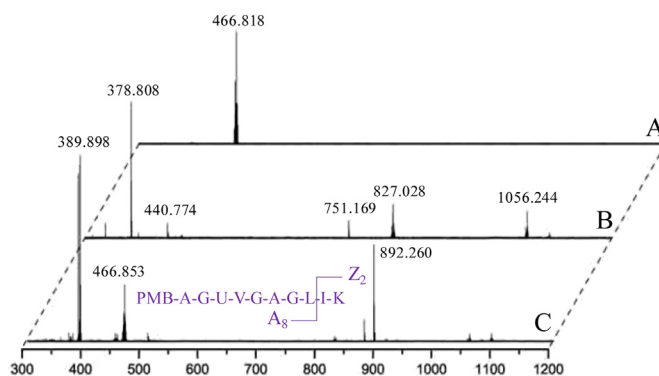


Fig. 6. MALDI-TOF-MS of (A) compound **2c**, (B) model peptide PMB-AGUVGAGLIK, and (C) model peptide incubated with **2c** at a molar ratio of 1:1 at 37 °C for 18 h. A new molecular ion peak appears at m/z 892.260 that is attributed to addition of 1 Se atom to the 8-residue peptide fragment PMB-AGUVGAGL (A_8), while another new fragment peak appears at m/z 389.898 that is due to fragment of compound **2c** that loss a Se atom.

blot analysis was also performed to further examine the expression level of TrxR and generation of Trx. The results (Fig. 5B) showed that exposing A375 cell lines to 8 Gy alone caused increase in the expression level of Trx protein. Nevertheless, there was a significant decline in the Trx expression when exposed to **2c**. In addition, exposing cells to **2c** alone or in combination with 8 Gy witnessed no dramatic alteration in expression level of TrxR. So, this demonstrated that **2c**-induced inhibition on TrxR might be the major contributing factor in the cell apoptosis as well as solving the problem of ionizing radiation induced resistance.

2.8. 1,2,5-Selenadiazole-peptide interactions

To obtain further insight on the occurring 1,2,5-selenadiazole-protein interactions on the molecular level, a MS strategy similar to that described by Lu et al. [22] was applied relying on MS determinations. Thus, MALDI ToF MS analysis was carried out on pre-reduced TrxR model peptide PMB-Ala-Gly-Sec-Val-Gly-Ala-Gly-Leu-Ile-Lys (PMB-AGUVGAGLIK) treated with **2c** (1:1 ratio) for 18 h at 37 °C. As shown in Fig. 6A–C, the dramatic decline in the molecular ion peak of **2c** and nearly vanished peak of model peptide suggest that the interaction between compound **2c** and the model peptide indeed carried out. MS analysis led to a new molecular ion at m/z 892.26, which corresponds to a single Se atom assigned to the 8-residue peptide fragment PMB-AGUVGAGL. This can be further confirmed by the new fragment peak at 389.898, which was just attributed to loss of a Se atom from compound **2c**.

All these alteration can provide evidence sufficient to support the claim that leucine residue as the major Se binding site.

3. Conclusions

Selenadiazole derivatives have been identified as novel anti-proliferative agents in CRT against A375 cancer cells, which can result in distinct apoptosis-inducing activity via mitochondria-mediated, caspase-dependent and ROS-promoted apoptotic pathways. The results demonstrated the binding sites between 1,2,5-selenadiazoles and the model peptide of TrxR, suggesting that **2c** can be a potent agent in CRT for radiation-resistant human melanoma cells by targeting TrxR. This also provide valuable mechanistic clues for the design and synthesis of selenadiazole-oriented derivatives based on structure–activity relationships, giving a direction for further research on apoptosis-inducing or TrxR-targeting agents.

4. Experimental section

4.1. Synthesis of 1,2,3-thiadiazole derivatives (**1a**, **2a**, **2b** and **2c**)

Commercially available 3, 3'-Diaminobenzidine was utilized as starting material. A solution of 3, 3'-Diaminobenzidine (214 mg, 1 mmol) and selenium dioxide (111 mg, 1 mol) in 0.2 N HCl (30 ml) was stirred for 2 h at room temperature. Product was filtered, vacuum dried and separated by silica gel and eluted using CH₂Cl₂/CH₃OH (pure CH₂Cl₂-1:1) as eluent to gain **1a**. Yield: 91%. A mixture of **1a** (290 mg, 1 mmol), p-TSA (17 mg, 0.1 mmol) and 3,4,5-trimethoxybenzaldehyde (235 mg, 1.2 mol) was dissolved in DMF (60 ml). The mixture was stirred at 80 °C for 2 h. DMF was evaporated, leaving a residue which was washed with water (3 × 30 ml), vacuum dried, monitoring by TLC (GF254, Qingdao Haiyang Chemical Co., Ltd. Qingdao) the residue was separated over silica gel column using CH₂Cl₂/CH₃OH (pure CH₂Cl₂-150:1–10:1) as eluent to afford fraction 1 and compound **2c** (yield: 46%). Fraction 1 was further subjected to reversed-phase HPLC (Agilent Edipse XDB-C18, 21.2 × 250 mm, 7 μm) on a C₁₈ column, using water and acetonitrile from 72:28 to 36:64 (8.0 ml/min) as mobile phase and ultraviolet as detector (320 nm) to gain **2a** (yield: 22%) and **2b** (yield: 18%).

4.2. Cell culture and irradiation

The human melanoma cells A375 cell line was purchased from American Type Culture Collection (ATCC, Manassas, VA) and cultured in DMEM medium, which was enriched with 10% fetal bovine serum, 100U/ml penicillin and 100 μg/ml streptomycin. In a humidified environment of 5% CO₂ atmosphere at 37 °C the cells were incubated and subcultivated twice a week. Cell lines were irradiated with 8 Gy at a dose rate of 1.5 Gy/min using an Elekta Precise linear accelerator machine in room temperature.

4.3. Drug treatment

A375 cells were seeded in 96 well-plates at a density of 4×10^4 cells, allowed to grow to 70–80% confluence cells and incubated with different concentrations of **2a**, **2b** or **2c** (0, 1, 2, 4, 8, 16, 32 μg/ml) for 6 h, then irradiated with a dose of 0 Gy or 8 Gy X-ray under ambient conditions and further incubated at 37 °C for another 12 h (5% CO₂).

4.4. MTT assay

The cell viability was determined by MTT assay as previously described [23]. Briefly, after 18 h treatment, 30 μg/ml per well of MTT solution (5 mg/ml in PBS) was added and incubated for 4 h, the

medium was carefully aspirated and then replaced with 150 μl/well of DMSO to solubilize the formazan salt. After shaking for 20 min at room temperature, the plates were read with a microplate spectrophotometer (VersaMax) at 570 nm. The cell proliferation and viability was expressed as percentage of control (as 100%), each experiment was repeated on three occasions.

4.5. Flow cytometric analysis

A375 cells were treated with **2b** (10 μg/ml) or **2c** (4 μg/ml) for 6 h and then were exposed or unexposed to 8 Gy X-irradiation and further incubated for another 12 h. After treatments cells were trypsinized, centrifugated and washed with PBS and went to harvest, and fixed in 5 ml ice-cold 75% ethanol overnight at –20 °C. The fixed cells were washed with PBS and stained with propidium iodide (PI) under dark condition, cells were shaken for 30 min at 37 °C in the dark [24]. Stained cells were analyzed using a flow cytometer (Beckman Coulter).

4.6. Measurement of ROS generation

The intracellular level of ROS causing by **2b** or **2c** in A375 cells was determined using the oxidation-sensitive fluorescent probe H₂DCF and DHE. The cells were cultured in 96-well plates (4×10^4 /well) for 24 h at 37 °C. Next, A375 cells were treated with different concentration of **2b** (8 or 16 μg/ml) or **2c** (2 or 4 μg/ml) for 6 h, after which cells were exposed or unexposed to 8 Gy X-irradiation, then incubated with 2.5 μM H₂DCF (10 μmol/l) or 2.5 μM DHE (10 μmol/l) and further incubated for another 30 min at 37 °C, protected from light [25]. After incubation, increase in fluorescence resulting from oxidation of H₂DCF to DCF (485 nm excitation/535 nm emission) or DHE to hydroethidium (480 nm excitation/610 nm emission) was measured in a fluorescence microplate reader (Tecan SAFIRE). Relative fluorescence intensity of treated cells was expressed as percentage of control (as 100%).

4.7. Activities of TrxR

A375 cells were exposed to **2c** (2 μg/ml) alone or in combination with 8 Gy X-irradiation and TrxR activity was measured using a Thioredoxin Reductase Assay Kit (Cayman) as per manufacturer's instructions. In this assay, TrxR catalyzes the reduction of 5, 5'-dithiobis (2-nitrobenzoic) acid (DTNB) with NADPH to 5-thio-2-nitrobenzoic acid (TNB²⁻), which generate a strong yellow color ($\lambda_{\text{max}} = 412$ nm). As other enzymes can also reduce DTNB in crude biological samples, hence, TrxR specific inhibitor is utilized to determine TrxR specific activity.

4.8. Binding studies in a model peptide

The model peptide PMB–AGUVGAGLIK was incubated with **2c** at a molar ratio of 1:1 at 37 °C for 18 h. MALDI-TOF-MS MS based assay was carried out as previously reported [26].

4.9. Caspases activities assay

Cells (1×10^6 cells/dish) were seeded in 10 cm dishes. After different treatments with **2c** (2 μg/ml) alone or in combination with 8 Gy X-irradiation, cells were collected, washed three times with PBS and lysed in RIPA buffer, no sooner were Cell lysates clarified by centrifugation at 12,000 rpm for 5 min than the clear lysates were measured for protein concentration and caspase activity [27]. Briefly, total protein (80 μg/well) were placed in 96-well plates and then 3 μl specific caspase substrates (Ac-DEVD-AMC for caspase-3, Ac-IETD-AMC for caspase-8 and Ac-LEHD-AMC for caspase-9) were

added. Plates were incubated at 37 °C for 2 h under dark condition and caspase activity was determined by fluorescence intensity with the excitation and emission wavelengths set at 380 and 440 nm respectively.

4.10. Western blot analysis

After different treatments with **2c** (2 µg/ml) alone or in combination with 8 Gy X-irradiation to A375 cells, the medium was aspirated and the cells washed with cold PBS, lysed in ice-cold RIPA buffer (50 mM Tris–HCl, 1% Triton X-100, 150 mM NaCl, 1 mM EGTA, 1 mM EDTA, 20 mM NaF, 100 mM Na₃VO₄, 0.5%NP-40, 1 mM PMSF, 10 mg/mL aprotinin, 10 mg/mL leupeptin, pH7.4), Protein concentrations of cell lysates were determined by a BCA protein assay kit (Pierce, Rockford, IL, USA). Each extract (50 µg protein) was fractionated by electrophoresis in an SDS-polyacrylamide gel and transferred to a nitrocellulose membrane. Membranes were blocked with 5% skimmed milk in Tris-Buffered-Saline with Tween (TBST) at room temperature for 2 h. After which the membranes were incubated with primary antibodies at 1:1000 dilutions in 5% skimmed milk for 10 h at 4 °C, washed with TBST for 30 min, then appropriate HRP-conjugated secondary antibody (1:2000 dilution) was added to the membranes, which were incubated at room temperature for 1.5 h. Membranes were washed three times with TBST for 15 min each. Protein bands were visualized on X-ray film using an enhanced chemiluminescence system (Kodak).

4.11. Statistical analysis

Experiments were carried out at least in triplicate and all the data is expressed as mean ± SD. One-way analysis of variance (abbreviated one-way ANOVA) was used in multiple group comparisons. All statistical analysis was performed using SPSS v.20 (IBM Corp.). Differences between two groups were analyzed by two-tailed Student's *t*-test. Difference with *P* < 0.05 (*) was considered statistically significant.

Acknowledgments

This work was supported by National High Technology Research and Development Program of China (863 Program, SS2014AA020538), Science Foundation for Distinguished Young Scholars (S2013050014667) of Guangdong Province, Natural Science Foundation of China (21271002, 21371076, 21201082) and Natural Science Foundation of Guangdong Province (S2012040006919), Research

Fund for the Doctoral Program of Higher Education of China (20114401110004) and China Postdoctoral Science Foundation.

Appendix A. Supporting information

Supplementary data related to this article can be found at <http://dx.doi.org/10.1016/j.ejmech.2014.07.032>.

References

- [1] P. Wardman, Clin. Oncol. U. K. 19 (2007) 397–417.
- [2] J. Brognard, A.S. Clark, Y. Ni, P.A. Dennis, Cancer Res. 61 (2001) 3986–3997.
- [3] E.I. Azzam, S.M. de Toledo, J.B. Little, Oncogene 22 (2003) 7050–7057.
- [4] A. Deorukhkar, S. Krishnan, Biochem. Pharmacol. 80 (2010) 1904–1914.
- [5] J.E. Biaglow, I.S. Ayene, C.J. Koch, J. Donahue, T.D. Stamato, J.J. Mieyal, S.W. Tuttle, Radiat. Res. 159 (2003) 484–494.
- [6] M. Diehn, R.W. Cho, N.A. Lobo, T. Kalisky, M.J. Dorie, A.N. Kulp, D. Qian, J.S. Lam, L.E. Ailles, M. Wong, B. Joshua, M.J. Kaplan, I. Wapnir, F.M. Dirbas, G. Somlo, C. Garberoglio, B. Paz, J. Shen, S.K. Lau, S.R. Quake, J.M. Brown, I.L. Weissman, M.F. Clarke, Nature 458 (2009) 780–783.
- [7] J.E. Biaglow, R.A. Miller, Cancer Biol. Ther. 4 (2005) 6–13.
- [8] Y. Luo, T. Chen, X.C. Huang, Y. Wang, Y. Wong, W. Zheng, Acta Chim. Sin. 70 (2012) 1295–1303.
- [9] T. Chen, W. Zheng, Y.S. Wong, F. Yang, Biomed. Pharmacother. 62 (2008) 77–84.
- [10] S.C. Barranco, M.M. Romsdahl, R.M. Humphrey, Cancer Res. 31 (1971) 830–833.
- [11] L. Beels, J. Werbruggen, H. Thierens, Int. J. Radiat. Biol. 86 (2010) 760–768.
- [12] X.-J. Jiang, M.-Q. Song, Y.-N. Xin, Y.-Q. Gao, Z.-Y. Niu, Z.-B. Tian, World J. Gastroenterol. 18 (2012) 1404–1409.
- [13] G.G. Steel, M.J. Peckham, Int. J. Radiat. Oncol. 5 (1979) 85–91.
- [14] X. Han, H. Ma, Y. Wang, Russ. J. Org. Chem. 44 (2008) 872–874.
- [15] D.E. Fisher, Cell 78 (1994) 539–542.
- [16] F.H. Igney, P.H. Krammer, Nat. Rev. Cancer 2 (2002) 277–288.
- [17] T.J. Fan, L.H. Han, R.S. Cong, J. Liang, Acta Biochim. Biophys. Sin. 37 (2005) 719–729.
- [18] D.D. Newmeyer, S. Ferguson-Miller, Cell 112 (2003) 481–490.
- [19] C.R. Geest, P.J. Coffey, J. Leukoc. Biol. 86 (2009) 237–250.
- [20] C.L. Limoli, A. Hartmann, L. Shephard, C.R. Yang, D.A. Boothman, J. Bartholomew, W.F. Morgan, Cancer Res. 58 (1998) 3712–3718.
- [21] J. Lu, L.V. Papp, J. Fang, S. Rodriguez-Nieto, B. Zhivotovsky, A. Holmgren, Cancer Res. 66 (2006) 4410–4418.
- [22] J. Lu, H.E. Chew, A. Holmgren, Proc. Natl. Acad. Sci. U. S. A. 104 (2007) 12288–12293.
- [23] A.H. Cory, T.C. Owen, J.A. Barltrop, J.G. Cory, Cancer Commun. 3 (1991) 207–212.
- [24] M.R. Betts, J.M. Brenchley, D.A. Price, S.C. De Rosa, D.C. Douek, M. Roederer, R.A. Koup, J. Immunol. Methods 281 (2003) 65–78.
- [25] O. Oldenburg, Q. Qin, T. Krieg, X.M. Yang, S. Philipp, S.D. Critz, M.V. Cohen, J.M. Downey, Am. J. Physiol. Heart Circ. Physiol. 286 (2004) H468–H476.
- [26] G. Chiara, M. Guido, S. Francesca, D. Barbara, P.R. Maria, B. Alberto, A.C. Maria, P. Giuseppe, M. Luigi, C. Angela, Med. Chem. Commun. 2 (2011) 50–54.
- [27] I. Tamm, Y. Wang, E. Sausville, D.A. Scudiero, N. Vigna, T. Oltsersdorf, J.C. Reed, Cancer Res. 8 (1998) 5315–5320.